JOURNAL OF VIROLOGY, June 2010, p. 6103–6118 Vol. 84, No. 12
0022-538X/10/$12.00 doi:10.1128/JVI.02042-09

Interplay of RNA Elements in the Dengue Virus 5′ and 3′ Ends Required for Viral RNA Replication▽

Peter Friebe and Eva Harris*

Division of Infectious Diseases and Vaccinology, School of Public Health, University of California, Berkeley, 1 Barker Hall, Berkeley, California 94720-7354

Received 28 September 2009/Accepted 19 March 2010

***Dengue virus* (DENV) is a member of the *Flavivirus* genus of positive-sense RNA viruses. DENV RNA replication requires cyclization of the viral genome mediated by two pairs of complementary sequences in the 5′ and 3′ ends, designated 5′ and 3′ cyclization sequences (5′-3′ CS) and the 5′ and 3′ upstream of AUG region (5′-3′ UAR). Here, we demonstrate that another stretch of six nucleotides in the 5′ end is involved in DENV replication and possibly genome cyclization. This new sequence is located downstream of the AUG, designated the 5′ downstream AUG region (5′ DAR); the motif predicted to be complementary in the 3′ end is termed the 3′ DAR. In addition to the UAR, CS and DAR motifs, two other RNA elements are located at the 5′ end of the viral RNA: the 5′ stem-loop A (5′ SLA) interacts with the viral RNA-dependent RNA polymerase and promotes RNA synthesis, and a stem-loop in the coding region named cHP is involved in translation start site selection as well as RNA replication. We analyzed the interplay of these 5′ RNA elements in relation to RNA replication, and our data indicate that two separate functional units are formed; one consists of the SLA, and the other includes the UAR, DAR, cHP, and CS elements. The SLA must be located at the 5′ end of the genome, whereas the position of the second unit is more flexible. We also show that the UAR, DAR, cHP, and CS must act in concert and therefore likely function together to form the tertiary RNA structure of the circularized DENV genome.**

Dengue virus (DENV), a member of the *Flaviviridae* family, is a human pathogen causing dengue fever, the most common mosquito-borne viral disease in humans. The virus has become a major international public health concern, with 3 billion people at risk for infection and an estimated 50 million dengue cases worldwide every year (28). Neither specific antiviral therapies nor licensed vaccines are available, and the biology of the virus is poorly understood.

DENV is a small enveloped virus containing a positive-stranded RNA genome with a length of approximately 10.7 kb. The virus encodes one large polyprotein that is co- and post-translationally cleaved into 10 viral proteins. The structural proteins C, prM/M, and E are located in the N terminus, followed by the nonstructural proteins NS1, NS2A, NS2B, NS3, NS4A, NS4B, and NS5 (6, 10). NS5, the largest of the viral proteins, functions as an RNA-dependent RNA polymerase (RdRP) (29). The coding region is flanked at both ends by untranslated regions (UTR). The 5′ end has a type I cap structure (m^7GpppAmp) mediating cap-dependent translation, but the virus can switch to a noncanonical translation mechanism under conditions in which translation factors are limiting (13). Cellular mRNAs are known to circularize via a protein-protein bridge between eIF4G and eIF4E (the cap binding complex) at the 5′ end and the poly(A) binding protein (PABP) at the 3′ end, enhancing translation efficiency. Despite the fact that the DENV 3′ UTR lacks a poly(A) tail, recent findings demonstrated binding of PABP to the 3′ UTR and an effect on RNA translation, suggesting a similar mechanism (12, 26).

In addition to a presumed protein-mediated genome circularization regulating viral translation, an RNA-RNA-based 5′ and 3′ (5′-3′) end interaction, which can occur in the absence of proteins, leads to circularization of the viral genome (1, 3, 4, 18, 20, 30, 33, 34). This cyclization of the genome is necessary for viral RNA replication, and thus far, two complementary sequences at the 5′ and 3′ ends have been identified (3). The first are the cyclization sequences (CS) present in the capsid-coding region at the 5′ end (5′ CS) and upstream of the 3′ stem-loop (3′ SL) in the 3′ UTR (3′ CS) (2, 4, 18, 20, 30). A second sequence, known as the 5′ upstream AUG region (5′ UAR) element in the 5′ UTR, base pairs with its complementary 3′ UAR counterpart, which is located at the bottom part of 3′ SL (1, 4, 30). Recently, the structure of the 5′ end of the DENV genome hybridized to the 3′ end was determined in solution (25), confirming previous computer-predicted structures for genome cyclization (4, 20, 30). Besides the base pairing between 5′-3′ UAR and 5′-3′ CS sequences, a third stretch of nucleotides was identified to form a double-stranded (ds) region between the 5′ and 3′ ends.

In addition to RNA sequences involved in 5′-3′-end interactions that are necessary for cyclization, the 5′ end of the viral genome harbors at least two more functional RNA elements, the stem-loop A (SLA) and capsid-coding region hairpin (cHP). The SLA consists of the first 70 nucleotides (nt) of the genome, forming a stable stem-loop structure. This structure has been confirmed in several studies and identified as a promoter element for RNA synthesis that recruits the viral RdRp NS5 (16, 22). Once NS5 is bound to the SLA at the 5′ end, it

* Corresponding author. Mailing address: Division of Infectious Diseases and Vaccinology, School of Public Health, University of California, Berkeley, 1 Barker Hall, Berkeley, CA 94720-7354. Phone: (510) 642-4845. Fax: (510) 642-6350. E-mail: eharris@berkeley.edu.

▽ Published ahead of print on 31 March 2010.

is believed to be delivered to the initiation site of minus-strand RNA synthesis at the 3′ end via 5′-3′ RNA-RNA circularization. In addition, a short poly(U) tract located immediately downstream of SLA has been shown to be necessary for RNA synthesis, although it is not involved in genome circularization (22). Finally, the cHP element resides within the capsid-coding region; it directs start codon selection and is essential for RNA replication (8, 9). The cHP structure is more important than its primary sequence. For start codon selection, it is believed that the cHP stalls the scanning initiation complex over the first AUG, favoring its recognition (9). In the case of RNA replication, the cHP likely stabilizes the overall 5′-3′ panhandle structure or participates in recruitment of factors associated with the replicase machinery (8).

In this study, we demonstrate that in addition to the 5′ CS and 5′ UAR sequences, a third stretch of nucleotides in the 5′ end is required for RNA replication and appears to be involved in genome circularization. This new motif is located downstream of the AUG and was therefore designated the downstream AUG region (5′ DAR) element, with the predicted counterpart in the 3′ end designated the 3′ DAR. Our results indicate that the 5′ DAR modulates RNA-RNA interaction and RNA replication, and restoring complementarity between the 5′ DAR and 3′ DAR rescues detrimental effects caused by mutations in the 5′ DAR on genome circularization and RNA replication. Although the role of the predicted 3′ DAR counterpart is less conclusive, it may serve to make other structures and sequences in the 3′ end available for 5′-3′ RNA-RNA interaction to facilitate the replication-competent conformation of the DENV genome.

Furthermore, we analyzed the functional interplay of RNA elements in the viral 5′ end, showing that two separate units are formed during replication. The first consists of the SLA, and it must be located at the very 5′ end of the genome. The second unit includes UAR, DAR, cHP, and CS elements, and the positional requirements are more flexible within the DENV RNA 5′ terminus. However, all four elements in the second unit must act in concert, forming a functional tertiary RNA structure of the circularized viral genome.

MATERIALS AND METHODS

Cell culture. Baby hamster kidney cells 21 clone 15 (BHK cells) were grown in minimal essential medium alpha (MEM-α; Gibco, Carlsbad, CA) with 100 U/ml penicillin, 100 μg/ml streptomycin, and 5% fetal bovine serum (FBS; HyClone, Logan, UT) at 37°C in 5% CO_2.

Construction of DNA plasmids. Unless otherwise stated, standard recombinant DNA technologies were used for all cloning procedures. The basic construct, pDRep, has been described previously (8) and was used to create the plasmid pDEN-5′UTR-Cap-tr (Fig. 1A), in which the DENV 5′ UTR and the first 72 nt of the capsid-coding region were fused to the encephalomyocarditis virus (EMCV) internal ribosome entry unit (IRES) separated by a short sequence carrying multiple stop codons for the various DENV 5′ start codons (9) and a multiple cloning site, including unique restriction sites for XbaI, PmeI, AgeI, SnaBI, and AscI. The sequence between the DENV capsid-coding sequence fragment and the EMCV IRES is 5′-TAACCCTAAAA**TCTAGA**ATA**GTTTAAAC**TA**CCGGTTACGTAGGCGCGCC**AT-3′, with recognition sites for restriction enzymes shown in bold. We also engineered the hepatitis delta virus ribozyme at the DENV 3′ end (19). To construct pDEN-5′UTR-Cap-tr-SPACER (Fig. 1A), we generated a PCR-based fragment containing approximatley 630 nt derived from the green fluorescent protein (GFP) gene (GenBank accession number GQ404376.1; position 3498 to 4126) and additional primer sequences, including SnaBI/AscI recognition sites, to insert the fragment into pDEN-5′UTR-Cap-tr. For pDEN-Cap-tr+5′UTR-Cap-fl, the DENV 5′ UTR and capsid sequence were amplified via PCR and inserted into pDEN-5′UTR-Cap-tr using XbaI/AgeI. For PCR-based mutations introduced into the 5′ sequences, a MluI restriction site upstream of the original T7 promoter and the newly engineered XbaI site were used to insert the modified fragments into pDEN-5′UTR-Cap-tr-SPACER. For PCR-based mutations introduced into the internally located 5′ UTR-Cap-fl sequence, the XbaI and AgeI sites were utilized to insert the mutated 5′ UTR and capsid sequence into pDEN-Cap-tr+5′UTR-Cap-fl. Primer sequences are available upon request.

***In vitro* transcription.** All DENV replicon DNA templates were generated by ClaI digestion of the corresponding plasmid, followed by phenol-chloroform extraction and ethanol precipitation. RNAs were generated by *in vitro* transcription using a RiboMax large-scale RNA production system (T7; Promega) with the following modifications to the manufacturer's protocol: 3 mM concentrations (each) of GTP, CTP, and UTP, 1 mM ATP, and 6 mM $m^7G(5')ppp(5')A$ cap analog (New England BioLabs, Beverly, MA) were incubated for 4 h at 37°C with the addition of 2 mM ATP after 30 min. Transcription was terminated by the addition of 2 to 3 U of RNase-free DNase (Promega) per μg of plasmid DNA and incubation for 30 min at 37°C, followed by acidic phenol-chloroform extraction and isopropanol precipitation. RNAs corresponding to the 5′ or 3′ viral ends were generated as described above, with the exception that 3 mM concentrations of each ribonucleoside triphosphate (rNTP) without $m^7G(5')ppp(5')A$ cap analog was used. Different DNA templates were derived by PCR based on the corresponding plasmid, using primer pair S_T7-50_MluI (5′-CATGCGCAC CCGTGGCCAGG-3′)/P_A-5′end (5′-GTTTCTCTCGCGTTTCAGCATAT TG-3′) for 5′ RNAs (for NoCS mutant 5′ RNAs, P_A-5′end-NoCS [5′-GT TTCTCTCGCGTTTGTCGTATAAC-3′] was used instead of P_A-5′end). For 3′ SL RNAs, templates were generated via PCR using primer pair S_EcoRI-T7-3′CS-3′SL (5′-AAGCTTGATATCGAATTCTAATACGACTC ACTATAGACCCCCCCGAAACAAAAAACAGC3-′) and P_A-3′end (5′-A GAACCTGTTGATTCAACAGCACC-3′), whereas for full-length 3′ UTR RNAs, templates were generated using primers P_S-3′end (5′-CGCAAATTTAATA CGACTCACTATAGGTAGAAAGCAAAACTAACATGAAAC-3′) and P_A-3′end. All RNAs were quantified spectrophotometrically, and the integrity was verified by electrophoresis on agarose gels.

RNA transfection and transient luciferase replication assays. Transfection of RNAs into BHK cells was performed as described previously (17); briefly, 5 to 10 μg of RNA transcript generated *in vitro* from DNA templates was mixed with 400 μl of a suspension of 10^7 BHK cells per ml in a cuvette with a gap width of 0.4 cm (Bio-Rad). After one pulse at 975 μF and 270 V with a Gene Pulser II system (Bio-Rad), cells were immediately transferred into 14 ml of MEM-α (Gibco). Two milliliters of the cell suspension was seeded per well of a 6-well plate and harvested at various time points. Cells were harvested using 500 μl 1× *Renilla* luciferase assay lysis buffer per well, and luciferase activity was measured using a *Renilla* luciferase assay system (Promega) and a GloMax-96 microplate luminometer (Promega) according to the manufacturer's instructions with slight modifications; namely, 50 μl cell lysate and 50 μl 1× *Renilla* luciferase assay substrate were used per sample.

RT-PCR for viral cDNA sequencing and qRT-PCR. Total RNA was prepared from transfected BHK cells at different time points after RNA transfection using an RNeasy mini kit (Qiagen). cDNA was obtained using a 5′/3′ rapid amplification of cDNA ends (RACE) kit, 2nd generation (Roche Applied Science), according to the manufacturer's instructions. The DENV-specific anti-sense primers used were RT-5 (5′-CTCCTAGTGAAAAGTTGTCGACC-3′), RT-6 (CAATGGTCTGATTTCCATCCCG), and RT-3 (5′-GGGGGGAGGGAGAG ATGGCG-3′). PCR fragments were subcloned into pCR2.1-TOPO (Invitrogen), and plasmid DNA was isolated by alkaline lysis. Sequencing was performed at the University of California, Berkeley, DNA Sequencing Facility. Quantitative reverse transcription-PCR (qRT-PCR) was performed as described previously (8) with NS5-specific primers and probe using TaqMan One-Step Master Mix (Applied Biosystems, Foster City, CA). RNA was normalized to cellular 18S RNA quantified using TaqMan VIC-MGB Primer Limited Eukaryotic 18S rRNA Endogenous Control (Applied Biosystems) in a parallel reaction. qRT-PCR was conducted using a Sequence Detection System 7300 (Applied Biosystems).

RNA binding assays. Uniformly ^{32}P-labeled RNA probes were *in vitro* transcribed as described above with minor modifications, using 1 mM rCTP and 50 μCi [α^{32}P]CTP. RNAs were heat denatured for 5 min at 95°C and slowly cooled to 70°C, followed by incubation on ice. RNAs (0.1 nM radioactively labeled 3′ RNA and 10 nM 5′ RNAs) were subsequently incubated in binding reaction buffer (5 mM HEPES [pH 7.5], 100 mM KCl, 5 mM $MgCl_2$, 3.8% glycerol, and 2.5 μg freshly added tRNA) at 37°C for 30 min to allow RNA-RNA complexes to form. RNA-RNA complexes were analyzed by electrophoresis through native 4.5% polyacrylamide gels supplemented with 5% glycerol. Gels were prerun for 30 min at 4°C at 125 V prior to sample loading using 0.5× Tris-borate-EDTA

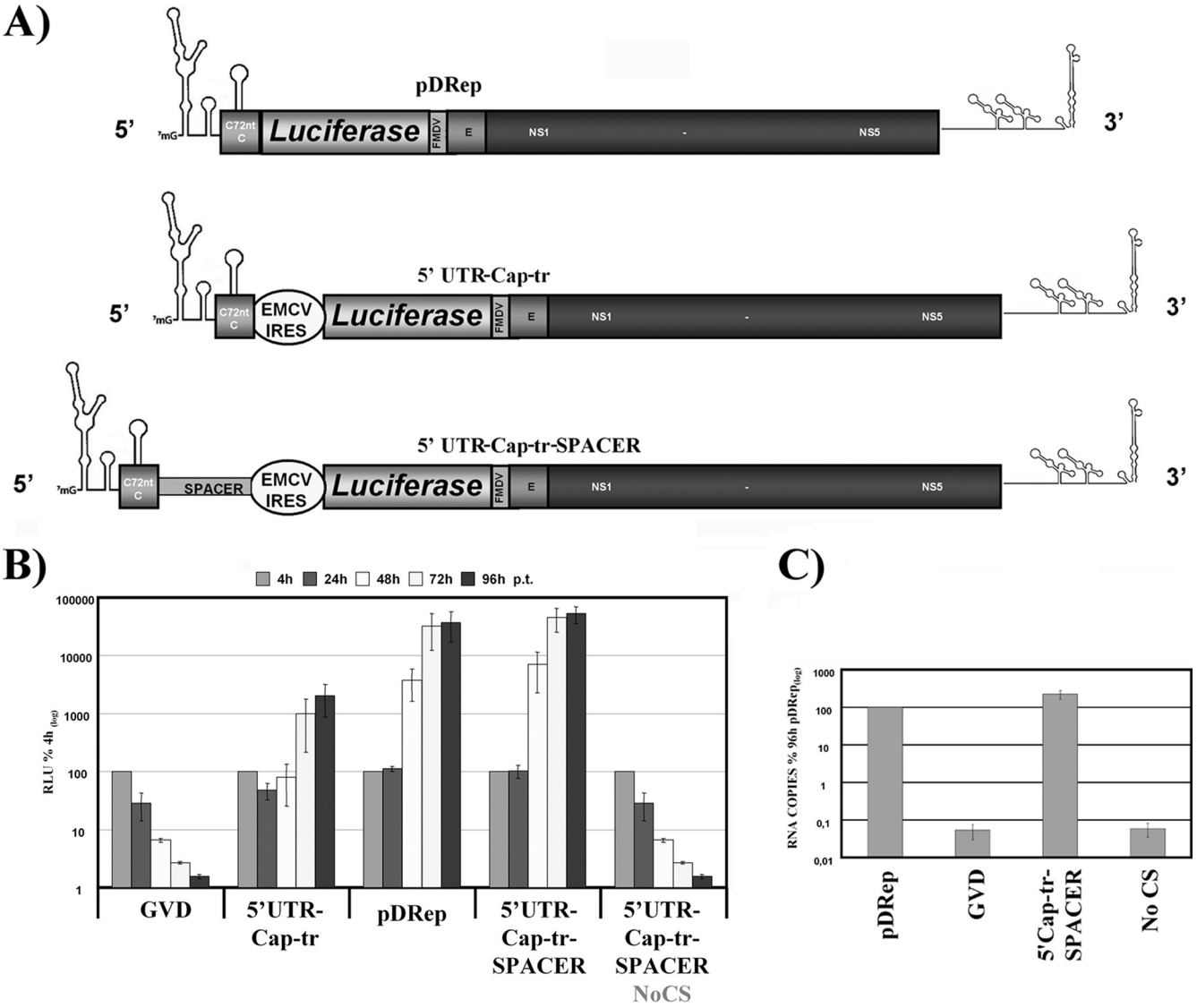

FIG. 1. Characterization of DENV reporter replicon. (A) Schematic presentation of the replicons used in this study. pDRep has been described previously (8). In 5′ UTR-Cap-tr, the EMCV IRES is positioned downstream of the DENV 5′ end containing the first 72 nt of the capsid-coding region (C72nt), mediating translation of *Renilla* luciferase (*Luciferase*) reporter gene and the viral open reading frame (ORF) spanning the C-terminal sequence of E and NS1 to NS5. Luciferase is cleaved from the viral proteins by an engineered FMDV2A (FMDV) cleavage site. RNA structures in the 5′ and 3′ ends are indicated schematically. In 5′ UTR-Cap-tr-SPACER, the DENV 5′ end and the EMCV IRES are separated by an ~650-nt-long spacer sequence derived from the GFP-coding sequence (SPACER). (B) Replication competence of DENV reporter replicons over a time course of 96 h posttransfection (p.t.). Time points are indicated on top, and RLU are expressed as a percentage of the value measured 4 h p.t., which was set to 100%. The replicons pDRep and GVD served as positive and negative controls, respectively. Results from at least three independent experiments are shown. Error bars reflect standard deviations. (C) Comparison of viral RNA copy number in BHK cells 96 h p.t. for the indicated replicon RNAs. RNA copy number was determined by qRT-PCR using NS5-specific primers and probe. The amount of viral RNA measured for the parental pDRep replicon was normalized to 18S RNA and set to 100%. All other normalized RNA levels are given as a percentage of pDRep. Results from at least three independent experiments are shown. Error bars reflect standard deviations.

(TBE) running buffer. Electrophoresis was carried out for 4 to 5 h at 4°C with constant voltage. Gels were dried at 80°C for 2 h and visualized by exposure on a PhosphorImager plate. Quantification was performed using ImageJ software (http://rsb.info.nih.gov/ij; developed by Wayne Rasband, National Institutes of Health, Bethesda, MD).

NS5 RdRP *in vitro* assays. RNAs used for RdRP assays were prepared as described above in "*In vitro* transcription." Prior to incubation with the recombinant purified NS5 RdRP domain (obtained from B. Selisko and B. Canard, Laboratoire AFMB, Marseille, France), RNAs were heat denatured as described for RNA binding assays. Five hundred nanograms of RNAs corresponding to 5′ and 3′ ends (the first 159 and last 456 nt, respectively) of the DENV genome were mixed in a modified RNA binding reaction buffer (5 mM HEPES [pH 7.5], 100 mM KCl, and 5 mM $MgCl_2$) and incubated for 30 min at 37°C. RNAs were than incubated with 250 nM recombinant purified NS5 in NS5 activity buffer (final concentration, 50 mM HEPES [pH 7.7], 5 mM $MgCl_2$, 5 mM $MnCl_2$, 2 mM [each] rATP, rUTP, and rGTP, 0.2 mM rCTP, 4 U RNase inhibitor, 5 mM dithiothreitol [DTT], and 5 μCi [α-^{32}P]CTP per reaction) for 1 h at 30°C. The reaction was stopped by buffer exchange with 10 mM Tris, and unincorporated nucleotides were removed by size exclusion chromatography using Micro Bio-Spin P-30 Tris columns (Bio-Rad). Prior to electrophoresis on a 6 M urea/5% denaturing polyacrylamide gel, RNAs were incubated at 65°C for 5 min in a 0.5× TBE buffer conataining 80% formamide. Products were visualized by exposure

on a PhosphorImager plate. As above, quantification was performed using ImageJ software (http://rsb.info.nih.gov/ij).

RESULTS

Bypassing the translational function of the 5′ UTR. To separate the effect of mutations introduced into the genomic 5′ end on RNA replication from their possible effect on translation efficiency and/or polyprotein expression, we constructed a reporter DENV replicon in which the requirements of 5′ RNA elements for RNA replication were uncoupled from translation of the reporter gene and the NS proteins required for RNA replication. The previously described reporter replicon pDRep (8) was modified by fusing the DENV 5′ UTR and the first 72 nt of the capsid-coding region followed by several stop codons to the EMCV IRES (Fig. 1A, pDRep and 5′ UTR-Cap-tr). The 5′ UTR and first 72 nt of the capsid-coding region harbor all essential 5′ RNA elements needed for autonomous RNA replication, and the engineered stop codons abort translation initiated at the 5′ AUG. The internal EMCV IRES mediates 5′-end-independent translation of the *Renilla* luciferase and the viral NS protein cassette, the latter of which is cleaved from the reporter via an engineered foot-and-mouth disease virus 2A (FMDV2A) cleavage site.

We tested the replication of the 5′ UTR-Cap-tr replicon compared to pDRep by transfecting the same amount of RNA of each construct into BHK cells and monitoring luciferase activity over a time course of 4 h, 24 h, 48 h, 72 h, and 96 h. The 4-h value, reflecting translation of the input RNA and thus serving as an indicator of transfection efficiency, was set to 100%, and all later values were normalized to the 4-h value to correct for transfection efficiency. For both replicons, total luciferase activity levels (in relative luciferase units; RLU) 4 h after transfection were similar (data not shown), indicating that 5′ cap-dependent (pDRep) and EMCV IRES-dependent (5′ UTR-cap-tr) translation levels are comparable in BHK cells. As a negative control, a replicon with an inactivating mutation (GDD to GVD) in the catalytic site of the NS5 RdRp was used (8). The replication phenotype of 5′ UTR-cap-tr was somewhat delayed compared to that of pDRep (Fig. 1B, 5′ UTR-Cap-tr and pDRep). That viral RNA elements derived from two different viruses fused to each other can interfere with their functionality was previously reported for other *Flaviviridae* (17). To overcome any steric constraints, we separated the DENV 5′ end and the EMCV IRES by an ~650-nt-long spacer derived from the GFP-coding sequence. Replication of the resulting replicon (Fig. 1A, 5′ UTR-Cap-tr-SPACER) was comparable to that of pDRep and was substantially enhanced compared to that of 5′ UTR-Cap-tr (Fig. 1B, 5′ UTR-Cap-tr versus 5′ UTR-Cap-tr-SPACER). To demonstrate the functionality of the new replicon system, we tested a replicon with a substitution of the CS sequence (5′-UCAAUAUGCUG-3′ to 5′-AGUUAUACGAC-3′) that abolishes 5′-3′ CS complementarity, which abrogated RNA replication (Fig. 1B, Cap-tr-SPACER-NoCS). The relation between luciferase activity and RNA levels for the new replicon design was confirmed by measuring the amount of viral RNA 96 h posttransfection (p.t.) (Fig. 1C).

The DAR sequences are involved in viral RNA replication. We recently confirmed the computer-predicted 5′-3′ cyclization structure by determining the solution structure of the 5′ end of the DENV genomic RNA hybridized to the 3′ end of the DENV genome (25). The overall structure confirmed the interaction between the 5′ and 3′ CS and UAR sequences, leading to a rearrangement of the 5′ and 3′ ends (Fig. 2A). The results also confirmed that the SLA is formed identically in the presence or absence of the 3′ RNA and that the cHP structure is only slightly altered at the bottom of the stem. The solution structure analysis also revealed a third double-stranded region, with 5-nt base pairing between the 5′ and 3′ ends (Fig. 2A, dotted frame, magnified on top). Thus, far, this potential circularization element has not been analyzed for its impact on the viral life cycle. Nucleotides involved in this base pairing at the 5′ end are located downstream of the start codon and thus were designated the downstream AUG region (5′ DAR); nucleotides at the 3′ end predicted to base pair with the 5′ DAR are referred to as the 3′ DAR. To address the functional role of this region in RNA replication, we used the 5′ UTR-Cap-tr-SPACER replicon as a backbone to avoid interference by the possible impact of introduced mutations on RNA translation. We first introduced mutations into the 5′ DAR and adjacent sequences (Fig. 3A, 5′ DAR-region-mut). These mutations completely prevented RNA synthesis (Fig. 3B, 5′ DAR-region-mut).

To analyze the impact of mutations in the 5′ DAR-region-mut RNA on 5′-3′ genome cyclization, we used a previously reported method to study DENV RNA-RNA interaction (4). This method involves an RNA binding assay in which the interaction between two RNAs, one representing the 5′ end and the other the 3′ end, can be investigated. The 5′ RNAs containing the first 160 nt of the DENV genome and the indicated mutation were *in vitro* transcribed, as was a radiolabeled 3′ wild-type (WT) RNA spanning the final 106 nt of the DENV genome. As previously shown (4), the 5′ WT RNA was able to form an RNA-RNA complex with the 3′ WT RNA, resulting in a shift of the radiolabeled 3′ RNA, whereas a 5′ RNA harboring a mutation in the CS sequence (5′-UCAAU AUGCUG-3′ to 5′-AGUUAUACGAC-3′) abolishing 5′-3′ CS complementarity did not shift the 3′ RNA (Fig. 3C, compare lanes 1, 2, and 3). The 5′ DAR-region-mut RNA failed to shift the 3′ RNA (Fig. 3C, lane 4). To further analyze the role of the DAR sequence in genome circulization, we tested RNAs with mutations in the sequence between the 5′ UAR and the 5′ DAR ("upstream DAR," 5′-AUGAAUAA-3′ into 5′-UACU UAUU-3′), RNAs with mutations only affecting the 5′ DAR motif (Fig. 3A, 5′ NoDAR), and RNAs with mutations between the 5′ DAR sequence and the cHP element ("downstream DAR," 5′-GAAA-3′ into 5′-CUUU-3′. Only mutations in the 5′ DAR sequence abrogated the long-distance 5′-3′ RNA-RNA interaction (Fig. 3C, lane 7), indicating that the 5′ DAR sequence is involved in 5′-3′ RNA-RNA communication.

Next, the predicted base pairing between the 5′ DAR and 3′ DAR for the 5′ NoDAR mutant was restored by introducing complementary mutations into the 3′ DAR sequence (Fig. 3A, 5′-3′ NoDAR). Restoring complementarity between the DAR sequences restored the ability of terminal RNAs to interact with each other (Fig. 3C, lane 10). However, mutations in the 3′ DAR allowed 5′-3′ RNA-RNA interaction with the WT 5′ RNA despite the fact that the predicted complementarity be-

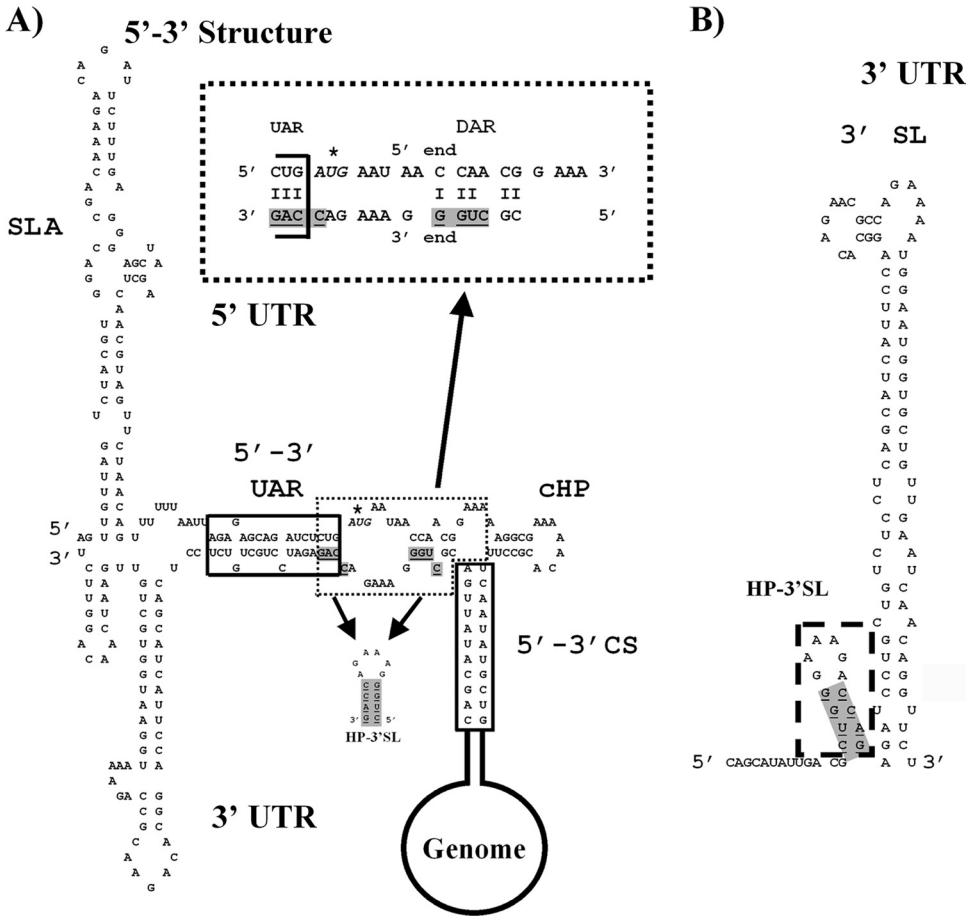

FIG. 2. Secondary structure of the DENV2 5′ end in the presence of the 3′ UTR and of the 3′ SL in the absence of 5′ RNA. (A) Interaction between the DENV 5′ and 3′ ends is depicted as determined from the solution structure of the 5′ UTR in the presence of the 3′ UTR (adapted from reference 25). Sequences derived from the DENV2 (strain 16681) 5′ end are on top, and those from the 3′ end are on the bottom. Structural elements are indicated (SLA, cHP), and known nucleotides required for 5′-3′ base pairing are boxed (5′-3′ UAR, 5′-3′ CS). The third double-stranded region between the 5′ and 3′ ends is surrounded by a dotted frame and magnified on top (DAR). Nucleotides involved in alternative stem formation at the 3′ end in the absence of 5′ RNA are underlined and shaded, and the structure itself is displayed below in 3′-5′ orientation (for details, refer to the legend to panel B). The start codon is highlighted in italics and marked with an asterisk. (B) Schematic presentation of the 3′ SL in the absence of 5′ RNA. The small stem-loop at the bottom of the 3′ SL is highlighted (dashed frame) and designated hairpin at 3′ SL (HP-3′ SL). Nucleotides involved in stem formation are underlined and shaded in all RNA structures (A and B).

tween the DAR sequences was abrogated (Fig. 3C, lane 9). Regardless of their ability to allow 5′-3′ RNA-RNA interaction, none of the mutants were able to initiate RNA replication in the context of our replicon system in BHK cells (Fig. 3B). While the loss of RNA synthesis by mutations in the 5′ DAR sequence could be explained by interference with genome circularization, the loss of RNA replication by RNAs with mutations in the 3′ DAR element might be explained by their effect on the formation of an alternative RNA structure, a small stem-loop at the bottom of the 3′ SL (Fig. 2A, underlined and with a grey background and shown as a structure beneath, and Fig. 2B, dotted frame). Because of its character and location, we will refer to this RNA structure as hairpin at the 3′ SL (HP-3′ SL). Previous results suggest a functional role for the HP-3′ SL in RNA replication (1).

To analyze whether the DAR and the HP-3′ SL are involved in regulating the NS5 RdRp, we performed an NS5 RdRp *in vitro* activity assay. Small RNAs derived from the DENV 5′ end are efficiently used as a template by purified NS5 RdRp *in vitro*, whereas the 3′ UTR RNA is recognized only in the presence of the 5′ end sequence (16, 22). It has been shown that for *trans*-initiation activity, the 5′ SLA RNA element and the presence of 5′-3′ CS and UAR complementarity, but not the primary sequence, are absolutely essential (1, 2). To analyze the effect of the 5′ DAR sequence and the HP-3′ SL element on NS5 RdRp *trans*-intiation, we used two RNAs corresponding to the viral ends with mutations in either the 5′ DAR or the 3′ DAR or both. For the 5′ end, we used RNA molecules consisting of the first 160 nt of the DENV genome, which are all recognized as a template by the purified RdRp independent of the introduced mutations (Fig. 3D). The corresponding 3′ UTR RNAs alone are not used as templates by purified NS5 RdRP protein *in vitro* (lane 1, WT 3′ UTR, and data not shown). The NS5 RdRP *trans*-initiation assay largely reflects the RNA-RNA hybridization results. While the 5′ NoDAR mutation abrogates RNA-RNA interaction and greatly decreases NS5 RdRp *trans*-initiation (Fig. 3D, lane 5), no significant effects were observed with RNAs containing

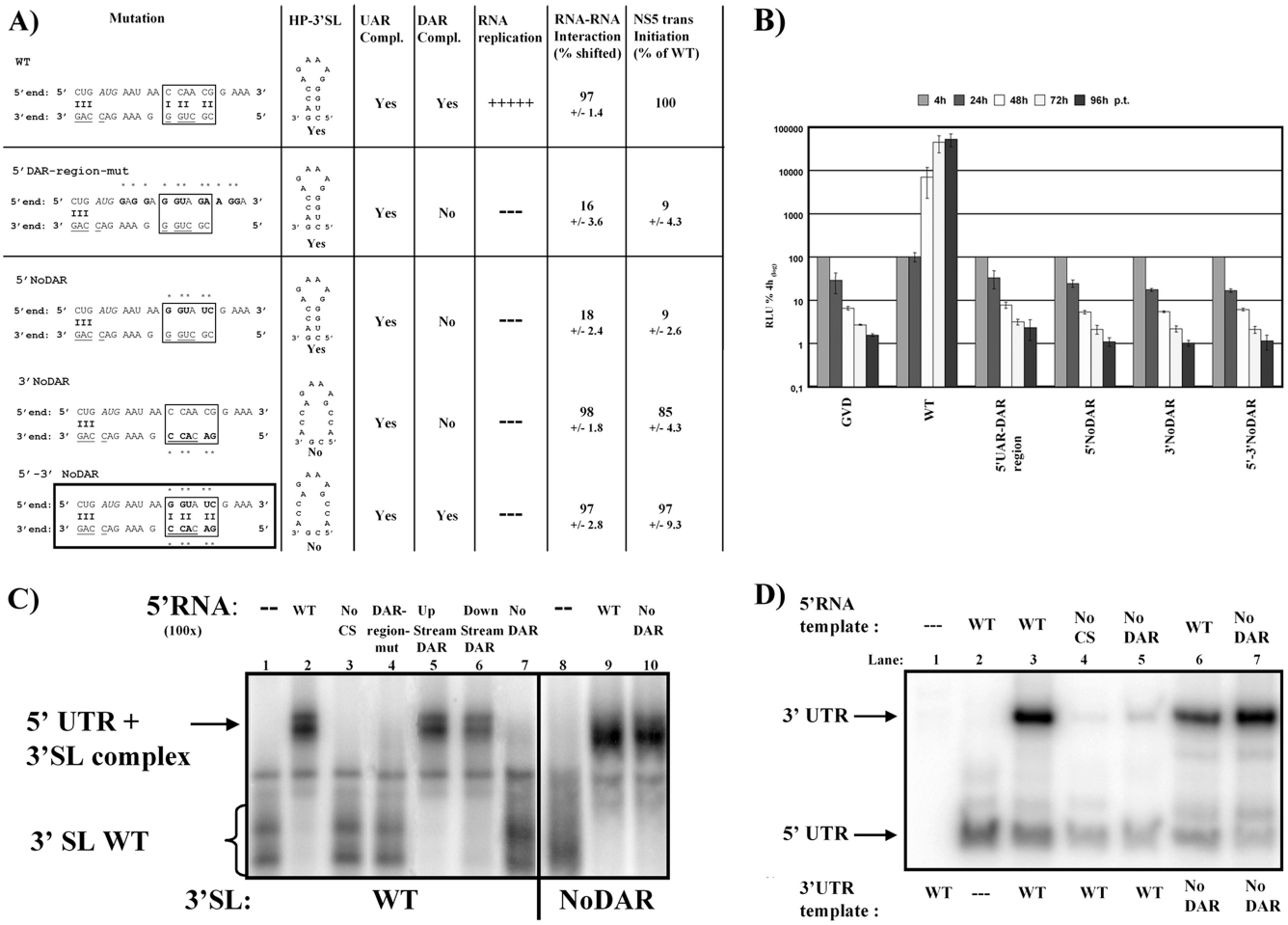

FIG. 3. The DAR sequences are important for RNA replication. (A) Overview of mutations and assay results. Detailed overview of mutations introduced into the 5′ UTR-Cap-tr-SPACER replicon are presented on the left side. The names of the mutants are indicated on top, with the other sequence as WT unless it is indicated that both the 5′ and 3′ mutant sequences are presented. Complementary nucleotides between 5′ and 3′ ends are indicated by a dash, and nucleotides involved in HP-3′ SL formation are underlined. The DAR motif is boxed. Mutations are highlighted with an asterisk. Mutants with restored complementarity between 5′-3′ DAR sequences are boxed. Prediction of HP-3′ SL formation is given in the column "HP-3′ SL" for each mutant. RNA replication levels are summarized with up to five plus signs, and no replication is shown with dashes; please refer to the legend to panel B for more details. Results regarding 5′-3′ RNA-RNA interaction and NS5 *trans*-initiation activity for each mutant are given as percentages of the quantified amount of 3′ RNA shifted (RNA-RNA interaction) or 3′ RNA synthesized compared to the 5′-3′ WT control. Values reflect mean values from at least three independent experiments, with the standard deviation (SD) shown immediately below. (B) Replication competence of variant DENV reporter replicons. RLU was measured over a time course of 96 h after transfection of variant replicons harboring the mutations indicated below the graph. For more details, refer to the legend to Fig. 1B. (C) RNA mobility shift analysis showing the effect of mutations within the 5′ and 3′ DAR and nearby sequences. Detailed overview of mutations are given in (A); mutant upstream DAR and downstream DAR contain the following 5′ sequence (limited to the sequence shown in panel A): 5′-CUG**UACUUAUU**CCAACG**GA**AA-3′ and 5′-CUGAUGAAUAACCAACG**CUUU**-3′; DAR sequences are underlined, mutations highlighted in bold). The 5′ RNA consists of the first 160 nt of the DENV genome, containing the mutations indicated along the top of the gel. The uniformly labeled 3′ SL RNA includes the final 106 nt of the DENV RNA genome, and the mutations are indicated below the gel. The ratio between the 5′ and 3′ RNAs was 100:1. The mobility of the 3′ SL alone or in complex with 5′ RNA is indicated on the left. The gel displayed is representative of results of at least three independent experiments. (D) Effects of mutations on RNA template usage and *trans*-initiation of RNA synthesis by purified RdRp. The gel displays the radiolabeled products from *in vitro* RdRp activity assays using the recombinant DENV NS5 RdRp domain. Mutations in the RNAs used as template (0.5 μg each) are indicated below (3′ UTR RNA template) and above (5′ UTR RNA template, corresponding to the first 160 nt) the gel. The migration pattern of the DENV 5′ UTR and 3′ UTR RNAs, as determined using the corresponding 5′ or 3′ *in vitro*-transcribed WT RNAs, are indicated on the left. Results displayed are representative of results of at least three independent experiments.

mutations in the 3′ DAR sequence (Fig. 3D, lanes 6 and 7). The results indicate no effect of the HP-3′ SL on the activity of the NS5 RdRp domain used in the assay.

Even though no direct effect of the HP-3′ SL on RdRp activity was seen, this does not rule out a functional role of this RNA element in RNA replication in the context of the entire genome or in the more complex environment in cells. To analyze whether the loss of RNA replication of replicon RNAs harboring the 3′ NoDAR mutation was due to interference with HP-3′ SL formation, we introduced additional mutations into the 3′ sequence to restore the formation of the HP-3′ SL. In the 3′ NoDAR mutation, 3 of 4 nt involved in formation of the HP-3′ SL stem are mutated, and most of the complementary nucleotides on the other side of the stem are bifunctional,

forming part of the HP-3′ SL stem as well as the 3′ UAR sequence (Fig. 2A, nucleotides involved in stem formation are underlined and shaded). In addition to the 3′ NoDAR mutations, we introduced compensatory mutations on the other side of the HP-3′ SL stem to restore the possibility of stem formation (Fig. 4A, 3′ UAR-NoDAR). Two of these mutations are located at the 5′ end of the 3′ UAR sequence, partially disrupting 5′-3′ UAR complementarity. To eliminate any effects of UAR noncomplementarity, we also introduced two mutations into the 5′ UAR sequence of the 5′ NoDAR mutant (Fig. 4A, 5′ UAR-NoDAR), restoring UAR complementarity between the combined 5′ plus 3′ UAR-NoDAR mutant (Fig. 4A). Even so, none of the mutant RNAs allowed RNA replication in cell culture (Fig. 4B). As expected from our previous results, RNAs containing mutations in the 5′ UAR and 5′ DAR sequence are not able to interact with 3′ WT RNAs (Fig. 4A, 5′ UAR-NoDAR, and data not shown), while the analogous mutations in the 3′ RNA still shifted 5′ WT RNAs (Fig. 4A, 3′ UAR-NoDAR, and data not shown). Despite a stable RNA-RNA interaction between 5′ WT and 3′ UAR-NoDAR RNAs, the NS5 *in vitro* assay showed a reduced *trans*-initiation activity of the corresponding 3′ RNA templates (Fig. 4A, upper panel, and data not shown). Interestingly, combination of 5′ UAR-NoDAR and 3′ UAR-NoDAR RNAs showed a similar RNA-RNA interaction pattern but resulted in a restored NS5 trans initiation *in vitro* activity (Fig. 4A and data not shown).

Even though all UAR-NoDAR mutants maintain the possibility of forming the HP-3′ SL, none of the RNAs were replication competent (Fig. 4A, upper panel, and Fig. 4B). Therefore, to minimize the effects of mutating the DAR primary sequence on RNA replication, we constructed a set of mutants containing only 3 rather than 5 mutations in either DAR sequence and the same 2 mutations in the terminal UAR sequences as described above. Again, these UAR mutations were necessary to maintain the possibility of HP-3′ SL formation while maintaining 5′-3′ UAR complementarity, resulting in 5′ UAR-DAR-mut, 3′ UAR-DAR-mut, and 5′-3′ UAR-DAR-mut (Fig. 4A). To discriminate between effects on RNA replication caused by the changes in the UAR and DAR sequences, we also constructed an RNA harboring a mutation only in the 5′ UAR, which interferes only with 5′-3′ UAR complementarity, or mutations in the 5′ UAR in combination with the 3′ UAR-DAR-mut, which restore UAR complementarity and the possibility of forming the HP-3′ SL but lack DAR complementarity (Fig. 4A, 5′ UAR-only-mut and 5′ UAR + 3′ UAR-DAR-mut, respectively). The only RNA in this set that was able to replicate to some degree in cell culture contained restored 5′-3′ UAR and DAR complementarity (Fig. 4A and B, 5′-3′ UAR-DAR-mut), whereas all other mutants failed to replicate (Fig. 4B). Furthermore, two sets of RNAs again showed a discrepancy between 5′-3′ RNA-RNA binding ability and NS5 *trans*-initiation activity (Fig. 4A, 3′ UAR-DAR-mut and 5′ UAR-only-mut, and data not shown). Similar overall results were also obtained with mutant RNAs carrying 4-nt substitutions in either the 5′ DAR or 3′ DAR and one mutation each in the 5′ UAR and 3′ UAR sequences, resulting in nonviable replicons 5′ UAR-DAR-mut-2 (5′-CU**C***AUG*AAUAA**GG**AA**UC**-3′; mutations are indicated in bold and underlined, start codon in italics) and 3′UAR-DAR-mut-2 (3′-GA**GG**AGAAAG**CC**UC**AG**-5′) or in the viable mutant replicon 5′-3′ UAR-DAR-mut-2, carrying both the 5′ and 3′ substitutions (data not shown).

The low-replication phenotype of 5′-3′ UAR-DAR-mut and 5′-3′ UAR-DAR-mut-2 could be explained by either an impact of the altered primary sequence or combined effects of changes in the UAR and DAR sequences. To avoid effects on RNA replication caused by changes in the UAR, we targeted the nucleotides in the 3′ DAR that do not require changes in the UAR sequences to allow formation of the HP-3′ SL. We therefore focused on either the 5′ first two nucleotides or the 3′ final nucleotide of the 3′ DAR motif and also introduced the necessary mutations to maintain the formation of the HP-3′ SL (Fig. 5A, 3′ DAR-mut-1 and 3′ DAR-mut-2). We also engineered mutations in the analogous 5′ DAR positions (Fig. 5A, 5′ DAR-mut-1 and 5′ DAR-mut-2) so as to restore the predicted base pairing with 3′ DAR-mut-1 and -2, respectively (Fig. 5A, 5′-3′ DAR-mut-1 and 5′-3′ DAR-mut-2). While mutations introduced into the 3′ terminus caused only a minor impact on RNA replication, the analogous 5′ DAR mutations substantially interfered with RNA replication (Fig. 5B). The replication pattern of 5′ DAR-mut-1 might indicate the emergence of revertants; however, cDNA sequencing of samples harvested 96 h p.t. either failed or showed no conclusive result (data not shown). Most importantly, the complementary mutants in the 3′ end restoring 5′-3′ DAR complementarity rescued the effect of the 5′ mutations (Fig. 5B, 5′-3′ DAR-mut-1 and 5′-3′ DAR-mut-2, respectively). Similar to previous observations, mutations introduced into the 5′ DAR sequence interfered with the ability to bind the 3′ WT RNA, whereas mutations in the 3′ RNA displayed a less-severe effect (Fig. 5A). As seen for the RNA replication phenotypes (Fig. 5B), restoring complementarity between the DAR motifs also restored high-affinity RNA-RNA interaction (Fig. 5A, compare 5′-3′ DAR-mut-1 or -mut-2 with 5′ or 3′ DAR-mut-1 or -mut-2, and data not shown). The NS5 *trans*-initiation activity reflected the results of RNA-RNA interaction assays (Fig. 5A and data not shown).

The SLA must be located at the very 5′ end, whereas the 5′ UAR, DAR, cHP, and CS elements are less position dependent. Having shown that the 5′ DAR sequence is important for RNA replication, we wanted to define the position dependence of the elements at the viral 5′ terminus. In addition to the SLA, UAR, DAR, and CS, the 5′ end contains more functional RNA sequences: a short poly(U) tract and the cHP structure. However, the exact functions of these sequences are not yet known. To gain a better understanding of the RNA elements at the viral 5′ end, we analyzed the interplay between the elements, starting by studying effects on position. A panel of mutants was constructed, targeting the different RNA elements. For SLA, two mutants were designed, one disrupting the lower stem (previously designated stem 1 and 2 [22]) (Fig. 6, SLA lower stem) and the other targeting the loop sequence by introducing two known nonviable mutations (Fig. 6, SLA ML340) (16). The poly(U) tract was either extended to 20 U residues or replaced by stretches of either 10 G, C, or A residues (Fig. 6, poly(U)-20, poly(A)-10, poly(C)-10, and poly(G)-10). To interfere with the 5′ UAR and 5′ CS elements, sequences were exchanged with their complementary sequences, eliminating the possibility of base pairing with their 3′

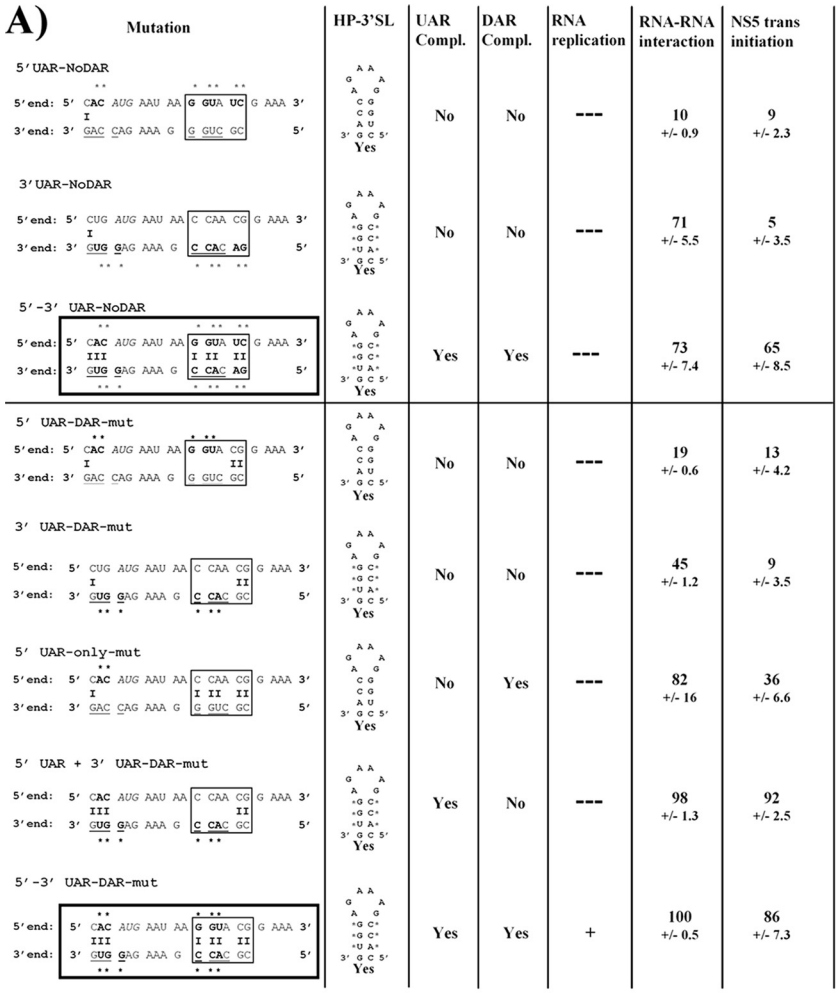

FIG. 4. Primary sequences and complementarity of the DAR elements and the HP-3′ SL are involved in DENV RNA replication. (A) Overview of mutations analyzed and results obtained. Detailed overview of mutations introduced into the 5′ UTR-Cap-tr-SPACER replicon on the left side, with names indicated on top. Please refer to the legend to Fig. 3A for more details. Mutants with restored complementarity between 5′-3′ UAR and DAR sequences are boxed. (B) Replication levels of indicated mutant replicons over a time course of 96 h p.t. For more details, see the legend to Fig. 3B.

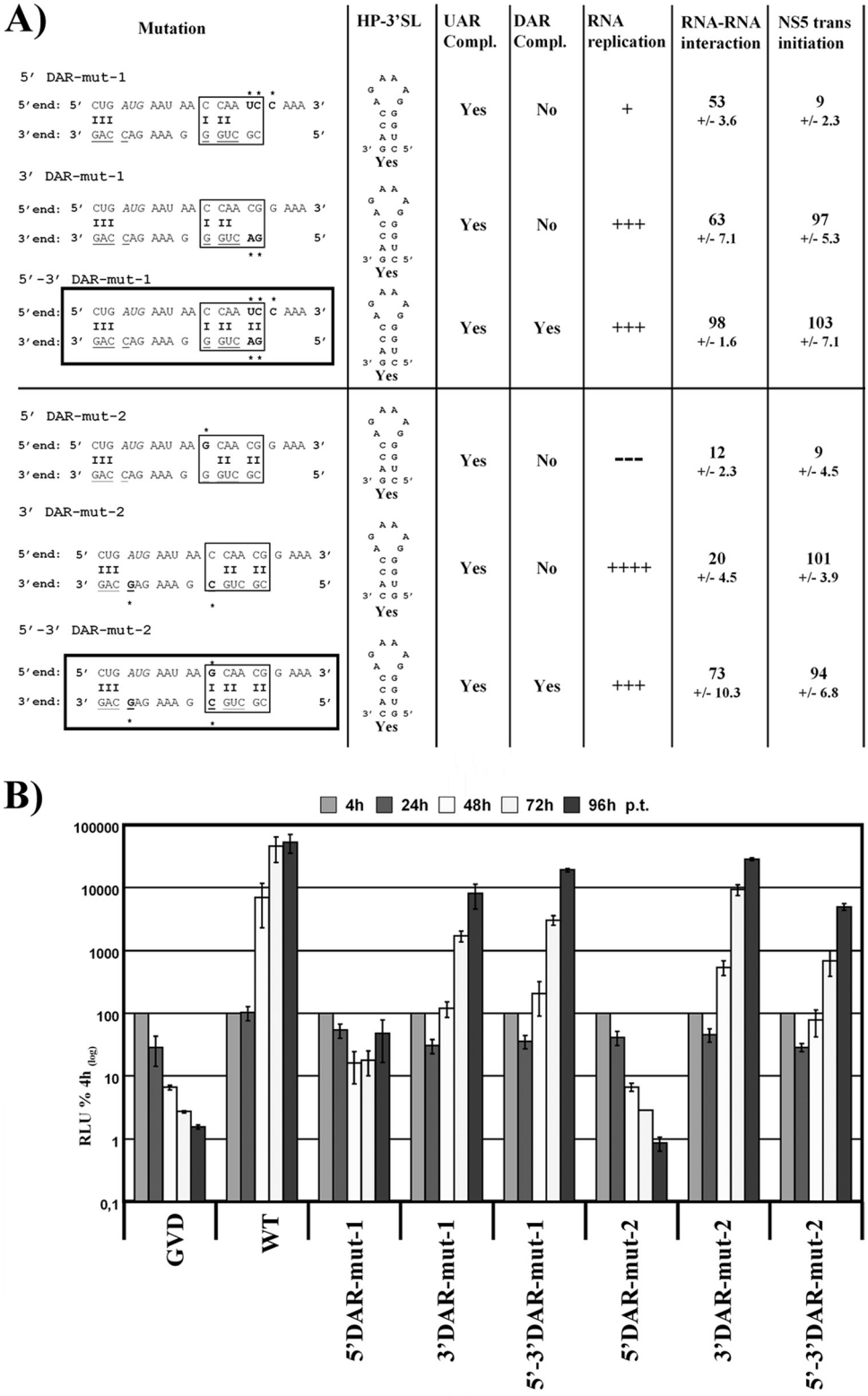

FIG. 5. Loss of replication due to 5′ DAR mutation can be rescued by restored DAR complementarity. (A) Overview of mutations and assay results. Detailed overview of mutations introduced into the 5′ UTR-Cap-tr-SPACER replicon on the left side, with names indicated on top. Please refer to the legend to Fig. 3A for more details. Mutants with restored complementarity between 5′-3′ DAR sequences are boxed. (B) Detailed replication levels of indicated mutant replicons over a time course of 96 h p.t. For more details, see the legend to Fig. 3B.

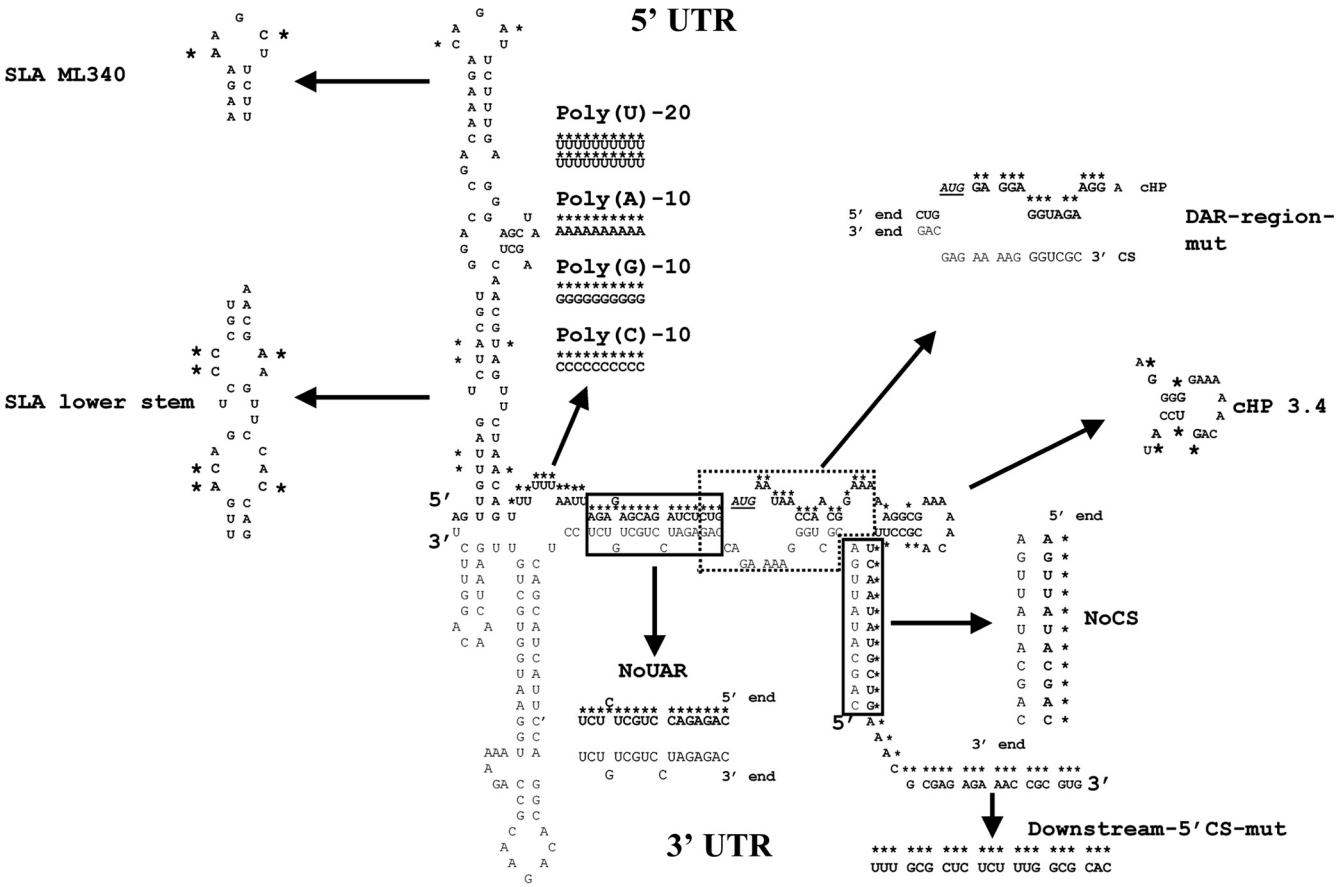

FIG. 6. Mutations introduced into the DENV 5′ end. The position of mutations within the 5′ end of the viral RNA are shown on top of the 5′-3′ RNA-RNA structure (see Fig. 2 for more details), indicated in bold and marked with an asterisk. The position of the mutations is further indicated by arrows, and the character of the mutations and their effects on RNA structure as predicted by mfold are shown, with mutated nucleotides marked with an asterisk. Names are indicated next to each mutation. Mutations were introduced only into the 5′ end. Mutated nucleotides are slightly enlarged. The start codon is shown in italics and underlined.

counterparts (Fig. 6, NoUAR and NoCS). For the DAR sequence, the DAR-region-mut mutant was selected, while for the cHP structure, a previously described mutation was used (Fig. 6, cHP3.4) (8). Finally, for mutant "downstream-5′ CS-mut" the first 21 nt 3′ of the 5′ CS element were exchanged with their complementary sequences (Fig. 6, Downstream-5′ CS-mut).

To test the effect on RNA replication, 5′ UTR-Cap-tr-SPACER replicons harboring the different mutations were transfected into BHK cells, and luciferase values were measured over a time course of 96 h to determine RNA replication levels. As expected, mutants NoCS and NoUAR and double mutant NoCS-NoUAR failed to replicate, as did the two replicons with changes in SLA known to interfere with RNA replication (Fig. 7A, non-viable). As previously described by Lodeiro et al. (22), an extension of the poly(U) tract or substitution with a poly(A) tract is well tolerated (reference 22 and Fig. 7A, viable); however, when replaced by a poly(C) or poly(G) tract, replication is blocked [Fig. 7A, non-viable, poly(C) and poly(G)]. Both the DAR-region-mut and the cHP3.4 mutations render the viral RNA replication incompetent. In the context of our new reporter replicons in which translation is uncoupled from the viral 5′ end, the loss of RNA replication of mutant cHP3.4 clearly demonstrated that the influence of the RNA element on RNA replication is independent from its role in RNA translation at all times during the viral life cycle. Mutations introduced into sequences downstream of the 5′ CS element do not interfere with viral RNA synthesis (Fig. 7A, viable, Downstream-5′ CS-mut).

To set up a system that allows analysis of the position effect of RNA elements within the 5′ region, we replaced the SPACER sequence from replicon 5′ UTR-Cap-tr-SPACER with an insertion of the 5′ UTR and the full capsid-coding region (Fig. 7B, top, 5′ UTR-Cap-tr+5′ UTR-Cap-fl). This replicon replicated to almost the same level as the parental 5′ UTR-Cap-tr-SPACER RNA (Fig. 7B, Control, compare WT with Cap-tr + 5′ UTR-Cap-fl), showing that the presence of two sets of 5′ RNA elements are well tolerated. Next, we analyzed whether the CS in the inserted sequence is able to functionally replace the homologous 5′ sequence by mutating the first 5′ CS to a NoCS mutation. In this setup, the 3′ CS sequence can only base pair with the internal CS element located approximately 180 nt downstream of its original position. The luciferase data shown in Fig. 7B (viable, NoCS) reveal an RNA replication rate similar to that seen for the parental RNA, indicating rescue of replication. However, 5′

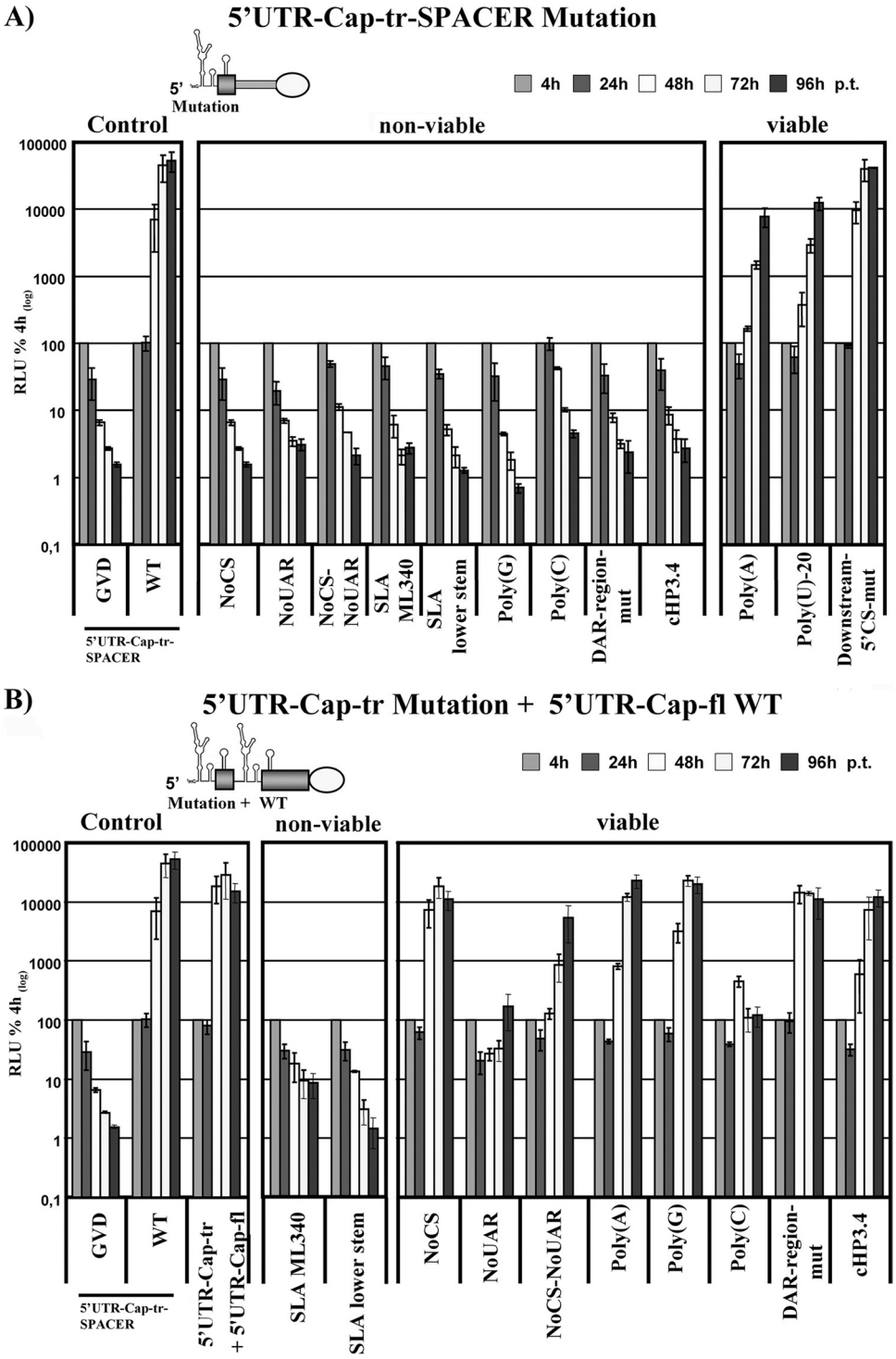

FIG. 7. The SLA is 5′-position dependent. (A) Effects of mutations in the 5′ end on RNA replication in the context of the 5′UTR-Cap-tr-SPACER replicon. RLU was monitored over a time course of 96 h. The name and a schematic diagram of the 5′ end of the replicon is provided above the graph, indicating the region into which mutations were introduced. The names of the mutants are provided below the graph. The results are clustered into sections containing controls (Control), RNAs with mutations that destroy replication competence (non-viable), and RNAs with mutations resulting in viable replicons (viable). For more details, please refer to legend to Fig. 1B. (B) Rescue of mutations in the 5′ end by internal insertion of the 5′ UTR and capsid-coding region. A schematic diagram of the 5′ end of the replicon is provided above the graph, and the region into which mutations were introduced is indicated. The replication competence of the mutants identified below the graph is shown. As described above, the results were clustered into control, viable, and nonviable replicon sections. For more details, refer to the legend to panel A.

UTR-Cap-tr-NoCS + 5′ UTR-Cap-fl contains a large sequence duplication that could allow the RNA to undergo recombination. Sequencing of cDNA clones confirmed the identity of viral RNAs 96 h p.t. as input sequence (data not shown). Taken together, these results demonstrate that mutations within the 5′ CS element can be rescued by an internal insertion, indicating that the RNA tolerates different positions close to the 5′ end for genome circularization.

Next, we tested whether the UAR element can also be functionally translocated by using the same setup. A 5′ NoUAR mutation can be rescued by an internal insertion, but replication is substantially delayed (Fig. 7B, viable, NoUAR). Due to the relatively close proximity of the SLA and UAR, reduction of RNA replication could be caused by effects of the introduced mutation on the 5′ SLA element, which cannot be compensated by an internal insertion, as described below. To reduce the likelihood of UAR mutation affecting the SLA, the poly(U) tract was extended to 20 poly(U) residues to act as a spacer sequence. However, no significant changes in the rescue levels were observed between the parental NoUAR and the poly(U)20-NoUAR RNA (data not shown). Therefore, we explored another explanation for the low-rescue phenotype. Recent results indicate that the CS sequences initiate the 5′-3′ long-distance RNA interaction (25), which could trap the 3′ CS base paired to the CS element at the 5′ end while formation of the cyclization structure is blocked by the NoUAR mutation. Therefore, we tested the rescue of a 5′ double mutant in which the 5′ UAR and CS elements are both mutated, such that the 3′ CS can only interact with the internal-rescue CS insertion, initiating end-to-end interaction close to the internal-rescue UAR sequence. This setup did improve restoration of RNA synthesis; however, viral fitness was not fully recovered (Fig. 7B, viable, NoCS-NoUAR), implying additional complexity. In line with the assumption of a more-complex effect of the NoUAR mutation on RNA replication is the fact that a mutation in the 5′ DAR sequence can be efficiently rescued (Fig. 7B, viable, DAR-region-mut; and UAR-DAR-mut, DAR-mut-1, and DAR-mut-2, data not shown). If rescue of the NoUAR mutation were reduced only due to a trapped 3′ end at the very 5′ end, the same should be true for DAR-region-mut rescue. Finally, mutation in the cHP element could be successfully rescued by an internal insertion (Fig. 7B, viable, cHP3.4).

As indicated above, the SLA does not allow functional relocation. None of the SLA mutations analyzed were rescuable by an internal insertion of the element (Fig. 7B, non-viable, SLA ML340 and SLA lower stem), indicating position dependency at the very 5′ end. Regarding the poly(U) region, while the replacement to poly(A) is accepted, substitution to either poly(G) or poly(C) tracts interfere with RNA replication. The poly(U)-to-poly(G) substitution could be efficiently rescued [Fig. 7B, viable, poly(G)], while the replacement of poly(U) with poly(C) was only partially rescued. Even after 96 h, only input luciferase values were attained [Fig. 7B, viable, poly(C)].

In order to further investigate the 5′ dependency of SLA, we repeated the rescue experiment with an insertion of the 5′ UTR plus the full capsid-coding region but lacking the SLA sequence. In this setup, only one 5′-located SLA is present and can be used by the virus to recruit NS5. As expected, mutations that could not be rescued before retained their nonviable phenotype (Fig. 8A, non-viable, SLA ML340), whereas all mutations efficiently rescued with a second SLA sequence present were also rescued in the absence of an internal SLA, demonstrating that all features of SLA are used at the 5′ position. However, the three mutants showing a low- or intermediate rescue phenotype with an additional SLA sequence inserted showed a no- or low-rescue phenotype in the absence of SLA in the 5′ UTR insertion [Fig. 8A, non-viable, NoUAR and poly(C); viable, NoCS-NoUAR]. Interestingly, in all three RNAs, the introduced mutations are in close proximity to the 5′ SLA sequence, and it is tempting to speculate that the mutations interfere with a feature of the SLA that can be rescued by an internal insertion, being 5′-end independent and explaining the partial rescue in the 5′ UTR-Cap-tr mutation plus 5′ UTR-Cap-fl backbone. This result indicates that the SLA may perform at least two independent functions, one that is completely 5′-end dependent and one that is somewhat more flexible in terms of position. Thus far, only the function of SLA in recruiting NS5 is known.

The 5′ end is divided into two functional units: the SLA and the UAR, DAR, cHP, and CS elements. Because a fully functional SLA element needs to be at the very 5′ end, whereas most of the other 5′ RNA elements can be translocated to an internal position, we wanted to determine which of the 5′-end elements must act in concert or can function individually. To address this question, a replicon setup was used carrying a NoCS mutation in the 5′ UTR and a mutated form of the RNA element of interest engineered into the 5′ UTR full capsid-coding sequence insertion. This design ensures that a functional copy of the RNA element of interest and the CS sequence are positionally separated.

The UAR sequence has already been reported to act together with the CS sequence to facilitate genome circularization (25), and we found that an RNA carrying a 5′ NoCS and an internal NoUAR mutation failed to replicate (Fig. 8B, non-viable, NoUAR), demonstrating the necessity for a direct interplay between both elements. The phenotype for replicon RNAs carrying the 5′ NoCS and the internal DAR-region-mut was expected to follow the fate of the NoUAR replicon but showed less of a decrease in luciferase activity (Fig. 8B, DAR-region-mut and UAR-DAR-mut) (and data not shown). Ninety-six hours after transfection, luciferase counts of these mutants were 10-fold higher than background levels, as determined using the replication-deficient GVD mutant. The luciferase kinetics observed could well be indicative of the emergence of revertants, although to date, cDNA sequencing of samples harvested 96 h p.t. have failed or shown no conclusive result (data not shown). Thus far, all mutations found have been at unique random positions, and their effect is as yet untested. A similar phenotype was observed for 5′ NoCS with the cHP3.4 mutation in the inserted rescue sequence (Fig. 8B, cHP3.4). This mutation has been previously analyzed and found to allow rescue revertants to arise, but in the context of an infectious clone (8). As already shown in Fig. 8A (NoCS), an RNA harboring the 5′ NoCS mutation and a deletion of SLA in the 5′ UTR insertion replicates to high levels (Fig. 8B, viable, No-SLA).

The substitution of the poly(U) tract to poly(G) in the inserted sequence abrogated RNA amplification, whereas a poly(C) tract was tolerated [Fig. 8B, non-viable, poly(G), and

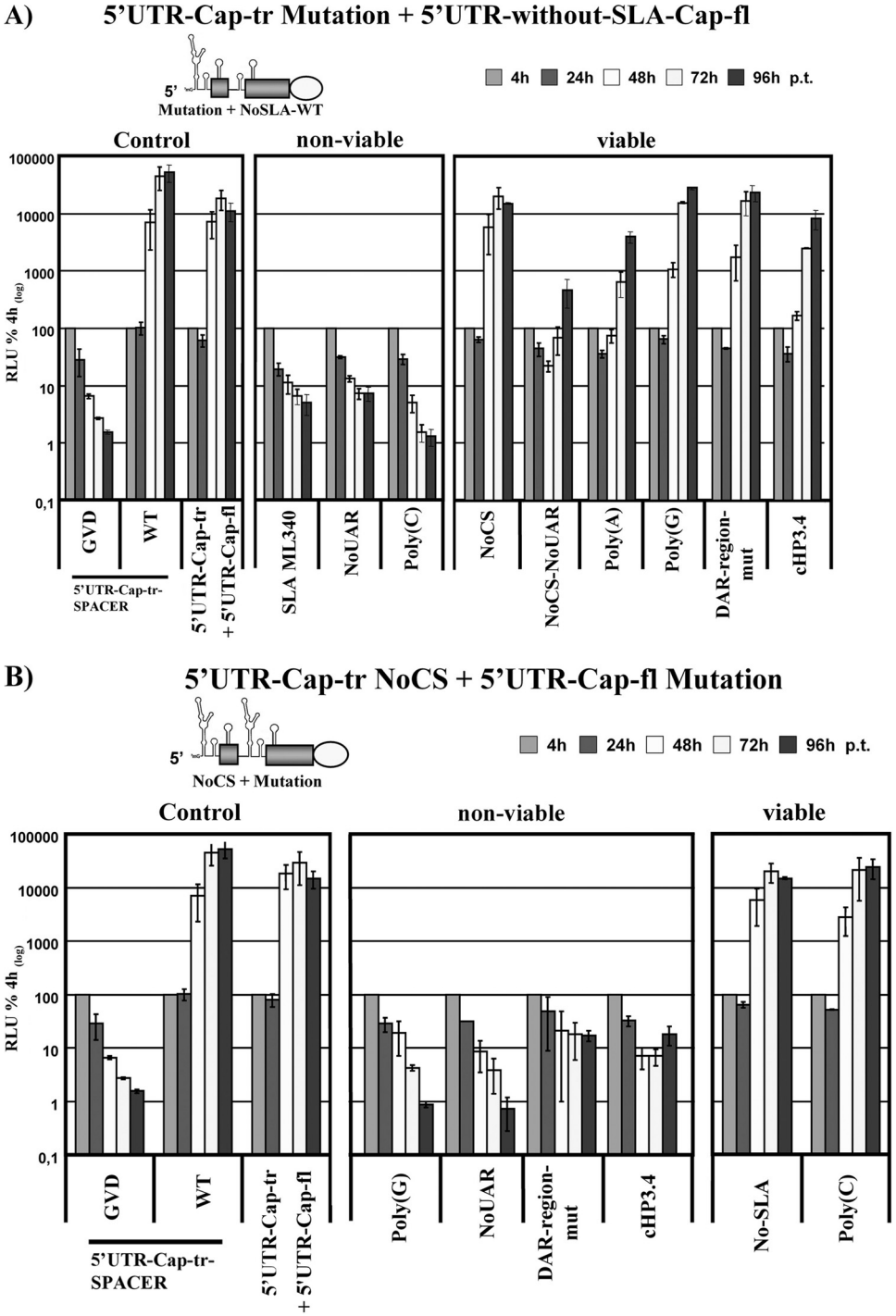

FIG. 8. Two functional units are present in the viral 5′ end: the SLA and the UAR, DAR, cHP, and CS elements. (A) Rescue of mutations in the 5′ end by internal insertion of the 5′ UTR and capsid-coding region without the SLA. A schematic diagram of the 5′ end of the replicon upstream of the EMCV IRES is provided above the graph, and the region into which mutations were introduced is indicated. For a more-detailed description, refer to the legend to Fig. 7. (B) Analysis of the interplay between different RNA elements in the 5′ end. A "NoCS" mutation is present at the very 5′ end, and the mutations indicated below the graph were engineered into the inserted 5′ UTR-capsid-coding sequence fragment; as before, a schematic overview is provided on top. For more details, please refer to legend to Fig. 7.

viable, poly(C)]. A possible explanation for these results could be an effect of the poly(G) but not the poly(C) substitution on the 5′-3′ RNA-RNA overall structure formation. In the case of the poly(C) substitution, possible effects on the internal SLA element could be compensated for by the intact 5′ SLA. To address the effect of the mutations on genome circularization, we performed RNA-RNA binding studies, studying the different mutations in the context of the first 160 nt of the viral

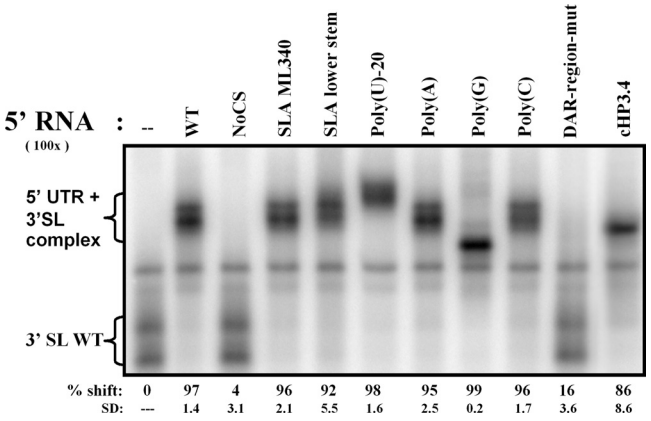

FIG. 9. Sequences outside the UAR, DAR and CS are not required for 5′-3′ RNA-RNA complex formation. RNA mobility shift analysis showing the effect of mutations within the DENV 5′ end on interaction with the 3′ end. The 5′ RNA consists of the first 160 nt of the DENV genome, carrying the mutations indicated on top of the gel. The uniformly labeled 3′ SL RNA includes the last 106 nt of the DENV genome. The ratio between the 5′ and 3′ RNAs was 100:1. The size of the 3′ SL alone or in complex with the 5′ DENV RNA is indicated on the left. The gel displayed here is representative of results of at least three independent experiments. For more details, refer to the legend to Fig. 3C.

RNA. Both the poly(G) and poly(C) replacements of the poly(U) tract did interact with the 3′ RNA; however, in the case of poly(G), a somewhat different mobility shift was observed [Fig. 9, poly(C) and poly(G)]. This could indicate formation of a nonfunctional 5′-3′ structure, which is also predicted by mfold-based RNA structure prediction (data not shown), showing that the introduced 5′ poly(G) tract is able to base pair with another poly(C) stretch found within the viral 3′ terminus. None of the other mutations located outside the circularization sequences interfered with the 5′-3′ RNA hybridization, except the DAR-region mutant (Fig. 9). Even though the cHP was found to be functional only within the 5′-3′ tertiary RNA structure complex, it is not required to initiate base pairings between sequences in the 5′ and 3′ ends. The cHP was also found to be dispensable in NS5 *trans*-initiation assays, indicating neither an impact on RNA hybridization nor NS5 promoter function *per se* (data not shown).

DISCUSSION

The impact of the UAR and CS elements on DENV genome circularization, which is essential for RNA replication, has been analyzed in several studies (1, 2, 4, 18, 20, 30, 33). Here, we report the impact of a third stretch of nucleotides (DAR) in the 5′ end impacting the long-distance RNA-RNA interaction and RNA replication. Although results regarding genome circularization for the complementary 3′ DAR sequence are less conclusive, this might be explained by the involvement of the 3′ DAR sequence in the formation of an alternative stem-loop structure (the HP-3′ SL) with nucleotides derived from the 3′ UAR element. Our data do provide evidence that the 3′ DAR sequence is important for RNA replication, either as a binding partner for the 5′ DAR or due to its involvement in the HP-3′ SL formation. We also show that two separate functional units are formed within the 5′ end: one consists of the SLA, and the other includes the UAR, DAR, cHP, and CS elements and is important for the formation of a functional 5′-3′ panhandle structure required for RNA replication.

Recently, the DENV 5′-3′ RNA-RNA structure was analyzed in solution (25); the results confirmed that the bottom half of the 3′ SL undergoes dramatic changes upon binding to the 5′ end of the viral RNA. It has been speculated that the 5′-3′ UAR interaction has two functions: stabilizing the 5′-3′ RNA-RNA hybridization complex and modulating the 3′ SL structure (16), under the hypothesis that these structural changes are required to make the 3′ end accessible for the viral RdRp, which is believed to function only with single-stranded RNA (ssRNA) (31). Because of the close proximity of the 3′ UAR and 3′ DAR elements and the fact that nucleotides from both elements are involved in the formation of the HP-3′ SL, it is tempting to speculate that the 5′-3′ DAR interaction assists the UAR element in unwinding the 3′ SL. In keeping with the fact that the CS sequences can initiate base pairing even in the absence of intact UAR complementarity, whereas the UAR interaction is more dependent on the presence of base pairing between the CS elements (25), the DAR element might extend the CS-initiated 5′-3′ interaction, thereby opening up the small HP-3′ SL at the bottom of the 3′ SL and making the 5′ nucleotides of the 3′ UAR accessible to the 5′ UAR sequence. This suggests a functional role for the structural changes at the 3′ end mediated by the 5′-3′ end interaction. In line with this assumption is the fact that for other plus-strand viruses, melting of the 3′ end RNA structure is a prerequisite for initiation of minus-strand synthesis (7, 24, 37, 38).

Even though our results regarding the influence of the 3′ DAR sequence on genome circularization are less clear than those obtained for the 5′ DAR, an explanation could be that mutations introduced into the 3′ DAR already influence the stability and/or formation of the HP-3′ SL and that, therefore, a 5′-3′ DAR interaction might not be needed to make the 3′ UAR accessible to the 5′ UAR. However, previous results indicated a role for the HP-3′ SL structure in RNA replication (1). This would result in a positive 5′-3′ RNA-RNA interaction but a block in RNA replication, as observed for mutants 3′ NoDAR, 3′ UAR-NoDAR, 5′ UAR + 3′ UAR-DAR-mut, 3′ UAR-DAR-mut, and 3′ UAR-DAR-mut-2. That mutations introduced into the 3′ DAR and adjacent sequences have an impact on 3′ RNA structure formation is supported by the different mobility patterns observed with mutant versus WT 3′ RNAs in the absence of 5′ RNAs (Fig. 3C, compare lane 1 [WT 3′ SL] with lane 8 [No DAR 3′ SL]; and data not shown for 3′ UAR-NoDAR, 3′ UAR-DAR-mut, 3′ DAR-mut-1, and 3′ DAR-mut-2). In addition, regarding the impact of the UAR elements on genome circularization, it has been shown that mutations in the 5′ UAR that disrupt 5′-3′ complementarity have a more severe effect on RNA replication than the analogous mutations in the 3′ UAR sequence (1). Furthermore, previous reports indicated that mutations in the 5′ UAR cause more severe effects on RNA-RNA interaction than the analogous mutations in the 3′ UAR (4). A similar mechanism would also explain the observed discrepancies between effects caused by mutations in the 5′ and 3′ DAR on genome circularization and RNA replication, while the observed rescue for

the combined 5′ and 3′ UAR-DAR-mut and UAR-DAR-mut-2 as well as the 5′ and 3′ DAR-mut-1 and DAR-mut-2 indicate a functional role for the predicted complementarity. The reduced replication levels for mutants with restored DAR complementarity indicate that the 5′ DAR primary sequence might also harbor a separate, as-yet-unknown function required for RNA replication.

Interestingly, some mutants showed a discrepancy between RNA-RNA affinity and NS5 *trans*-activity efficiency. Despite a high RNA-RNA affinity and no changes in SLA, NS5 *trans*-initiation of the 3′ RNA template for these mutants are reduced compared to the 5′-3′ WT RNA control. Mutations affect the complementarity of the UAR motifs overlapping with the sequences of the 3′ UTR involved in formation of the HP-3′ SL (3′ UAR-NoDAR, 3′ UAR-DAR-mut, and 3′ UAR-DAR-mut-2) or immediately adjacent nucleotides (5′ UAR-only-mut). These results might indicate not only that NS5 *trans*-initiation activity requires a stable 5′-3′ RNA-RNA interaction and functional formation of 5′-3′ panhandle complex but also that the WT primary sequences of the UAR regions in question are important.

The 5′ DAR sequence motif 5′-CCAACG-3′ is conserved in all four DENV serotypes, but not in other mosquito-borne flaviviruses, such as West Nile virus (WNV), Kunjin virus (KUN), or Japanese encephalitis virus (JEV). However, for these viruses, a sequence homologous to DAR is predicted to be present, and a conserved sequence equivalent to the DENV 5′DAR can be found located between the start codon and capsid hairpin element (5′-CCAGG-3′) (20, 35). The complementary DAR-like counterpart (5′-CCUGG-3′) at the 3′ end is also involved in formation of the small stem-loop structure at the bottom of the 3′ SL (23, 27, 36). Interestingly, a recent study using WNV NS5 showed that the protein binds to SL1, the homologous structure to the DENV SLA, together with upstream sequences, one of which is the WNV DAR-homologous 5′-CCAGG-3′ (11). In our study as well as in the study identifying SLA as the NS5 binding partner (16), only the RdRp domain of NS5 lacking the complete N-terminal RNA methyltransferase (MTase) domain was used; binding of the entire DENV NS5 might require RNA sequences in addition to those reported for the RdRp domain.

Our results strongly imply that in addition to the requirement of long-range RNA-RNA interaction to circularize the viral genome, the overall tertiary structure formed is also essential. All elements involved in RNA-RNA interaction between the viral termini must act in concert, forming a functional unit. Our data also show that the 5′ cHP RNA element, which is not involved in 5′-3′ RNA-RNA interaction *per se*, must be part of this unit to allow RNA replication to occur in cells. This result indicates that the 5′ cHP structure plays a role within the 5′-3′ RNA panhandle structure complex formed during cyclization. Our data did not reveal an impact of cHP on NS5 promoter activity, either when present in the 5′ end or within the 5′-3′ RNA-RNA complex. This is consistent with previous reports showing that the NS5 RdRp domain binds to SLA on the 5′ RNA alone and on the 5′-3′ RNA-RNA complex with similar affinities (16). Even though mutation of the cHP did not interfere with input replicon RNA translation in previous studies, an influence on translation during later steps in the viral life cycle affecting RNA replication could not formally be ruled out (8). Our new replicon design demonstrates that the influence of cHP on RNA replication is independent of its role in RNA translation at all times during the viral life cycle.

The SLA forms the second functional unit at the viral 5′ end. Structural requirements for SLA promoter properties have been studied in great detail (16, 22). Here, we show that the SLA is 5′-position dependent and does not tolerate translocation but that it does tolerate a positional separation of more than 150 nt from the other functional unit that forms an essential RNA tertiary structure required to cyclize the genome. However, the rescue pattern of some mutations in the poly(U) tract or the 5′ UAR with or without an internal SLA insertion implies that the SLA might contain a second function, which is more tolerant of translocation to an internal position within the 5′ region. Besides its role at the 5′ plus-strand end, the complementary sequence of nucleotides involved in SLA formation could also play a role at the 3′ end of the minus strand. In WNV, a role in binding of T-cell intracellular antigen 1 (TIA-1)/TIA-1-related protein (TIAR) to the RNA structure at the 3′ minus-strand end was demonstrated (21), and recently TIA-1/TIAR colocalization with DENV double-stranded RNA and the viral protein NS3 as well as a role in viral genomic RNA synthesis was reported (14, 15). It is believed that the viral 3′ minus-strand end serves as a promoter for plus-strand RNA synthesis, supported by reduction of RNA replication by peptide nucleic acids or RNA aptamers directed against the 3′ minus-strand end sequence of viruses from the *Flaviviridae* family (5, 32).

Taken together, our data demonstrates that a third stretch of nucleotides in the 5′ end of the DENV genome, designated the 5′ DAR element, is involved in the cyclization process and DENV RNA replication, and we have evidence that its predicted counterpart at the viral 3′ terminus (3′ DAR) is required for RNA replication due to its primary sequence or as part of the HP-3′ SL. Furthermore, all elements involved in 5′-3′ RNA-RNA communication as well as the cHP form a functional unit, necessary to circularize the viral genome and to form a functionally active tertiary RNA structure. A second separate unit is formed by the SLA, and nucleotides involved in the formation of SLA may fulfill at least two separate functions in the viral life cycle. This work further defines the complex interplay between RNA elements in the 5′ end and the 5′-3′ termini essential for DENV RNA replication.

ACKNOWLEDGMENTS

We gratefully acknowledge Bruno Canard and Barbara Selisko for purified DENV NS5 RdRp, Sondra Schlessinger for helpful discussions and editorial comments, and Simona Zompi for critical readings of the manuscript.

This work was supported by NIH grant AI052324 (E.H.).

REFERENCES

1. **Alvarez, D. E., C. V. Filomatori, and A. V. Gamarnik.** 2008. Functional analysis of dengue virus cyclization sequences located at the 5′ and 3′UTRs. Virology **375:**223–235.
2. **Alvarez, D. E., A. L. Lella Ezcurra, S. Fucito, and A. V. Gamarnik.** 2005. Role of RNA structures present at the 3′UTR of dengue virus on translation, RNA synthesis, and viral replication. Virology **339:**200–212.
3. **Alvarez, D. E., M. F. Lodeiro, C. V. Filomatori, S. Fucito, J. A. Mondotte, and A. V. Gamarnik.** 2006. Structural and functional analysis of dengue virus RNA. Novartis Found. Symp. **277:**120–132.
4. **Alvarez, D. E., M. F. Lodeiro, S. J. Luduena, L. I. Pietrasanta, and A. V.**

Gamarnik. 2005. Long-range RNA-RNA interactions circularize the dengue virus genome. J. Virol. **79:**6631–6643.
5. **Astier-Gin, T., P. Bellecave, S. Litvak, and M. Ventura.** 2005. Template requirements and binding of hepatitis C virus NS5B polymerase during in vitro RNA synthesis from the 3′-end of virus minus-strand RNA. FEBS J. **272:**3872–3886.
6. **Bartenschlager, R., and S. Miller.** 2008. Molecular aspects of Dengue virus replication. Future Microbiol. **3:**155–165.
7. **Chen, D., and J. T. Patton.** 1998. Rotavirus RNA replication requires a single-stranded 3′ end for efficient minus-strand synthesis. J. Virol. **72:**7387–7396.
8. **Clyde, K., J. Barrera, and E. Harris.** 2008. The capsid-coding region hairpin element (cHP) is a critical determinant of dengue virus and West Nile virus RNA synthesis. Virology **379:**314–323.
9. **Clyde, K., and E. Harris.** 2006. RNA secondary structure in the coding region of dengue virus type 2 directs translation start codon selection and is required for viral replication. J. Virol. **80:**2170–2182.
10. **Clyde, K., J. L. Kyle, and E. Harris.** 2006. Recent advances in deciphering viral and host determinants of dengue virus replication and pathogenesis. J. Virol. **80:**11418–11431.
11. **Dong, H., B. Zhang, and P. Y. Shi.** 2008. Terminal structures of West Nile virus genomic RNA and their interactions with viral NS5 protein. Virology **381:**123–135.
12. **Edgil, D., and E. Harris.** 2006. End-to-end communication in the modulation of translation by mammalian RNA viruses. Virus Res. **119:**43–51.
13. **Edgil, D., C. Polacek, and E. Harris.** 2006. Dengue virus utilizes a novel strategy for translation initiation when cap-dependent translation is inhibited. J. Virol. **80:**2976–2986.
14. **Emara, M. M., and M. A. Brinton.** 2007. Interaction of TIA-1/TIAR with West Nile and dengue virus products in infected cells interferes with stress granule formation and processing body assembly. Proc. Natl. Acad. Sci. U. S. A. **104:**9041–9046.
15. **Emara, M. M., H. Liu, W. G. Davis, and M. A. Brinton.** 2008. Mutation of mapped TIA-1/TIAR binding sites in the 3′ terminal stem-loop of West Nile virus minus-strand RNA in an infectious clone negatively affects genomic RNA amplification. J. Virol. **82:**10657–10670.
16. **Filomatori, C. V., M. F. Lodeiro, D. E. Alvarez, M. M. Samsa, L. Pietrasanta, and A. V. Gamarnik.** 2006. A 5′ RNA element promotes dengue virus RNA synthesis on a circular genome. Genes Dev. **20:**2238–2249.
17. **Friebe, P., V. Lohmann, N. Krieger, and R. Bartenschlager.** 2001. Sequences in the 5′ nontranslated region of hepatitis C virus required for RNA replication. J. Virol. **75:**12047–12057.
18. **Hahn, C. S., Y. S. Hahn, C. M. Rice, E. Lee, L. Dalgarno, E. G. Strauss, and J. H. Strauss.** 1987. Conserved elements in the 3′ untranslated region of flavivirus RNAs and potential cyclization sequences. J. Mol. Biol. **198:**33–41.
19. **Holden, K. L., D. A. Stein, T. C. Pierson, A. A. Ahmed, K. Clyde, P. L. Iversen, and E. Harris.** 2006. Inhibition of dengue virus translation and RNA synthesis by a morpholino oligomer targeted to the top of the terminal 3′ stem-loop structure. Virology **344:**439–452.
20. **Khromykh, A. A., H. Meka, K. J. Guyatt, and E. G. Westaway.** 2001. Essential role of cyclization sequences in flavivirus RNA replication. J. Virol. **75:**6719–6728.
21. **Li, W., Y. Li, N. Kedersha, P. Anderson, M. Emara, K. M. Swiderek, G. T. Moreno, and M. A. Brinton.** 2002. Cell proteins TIA-1 and TIAR interact with the 3′ stem-loop of the West Nile virus complementary minus-strand RNA and facilitate virus replication. J. Virol. **76:**11989–12000.
22. **Lodeiro, M. F., C. V. Filomatori, and A. V. Gamarnik.** 2009. Structural and functional studies of the promoter element for dengue virus RNA replication. J. Virol. **83:**993–1008.
23. **Olsthoorn, R. C., and J. F. Bol.** 2001. Sequence comparison and secondary structure analysis of the 3′ noncoding region of flavivirus genomes reveals multiple pseudoknots. RNA **7:**1370–1377.
24. **Olsthoorn, R. C., S. Mertens, F. T. Brederode, and J. F. Bol.** 1999. A conformational switch at the 3′ end of a plant virus RNA regulates viral replication. EMBO J. **18:**4856–4864.
25. **Polacek, C., J. E. Foley, and E. Harris.** 2009. Conformational changes in the solution structure of the dengue virus 5′ end in the presence and absence of the 3′ untranslated region. J. Virol. **83:**1161–1166.
26. **Polacek, C., P. Friebe, and E. Harris.** 2009. Poly(A)-binding protein binds to the non-polyadenylated 3′ untranslated region of dengue virus and modulates translation efficiency. J. Gen. Virol. **90:**687–692.
27. **Proutski, V., E. A. Gould, and E. C. Holmes.** 1997. Secondary structure of the 3′ untranslated region of flaviviruses: similarities and differences. Nucleic Acids Res. **25:**1194–1202.
28. **Swaminathan, S., and N. Khanna.** 2009. Dengue: recent advances in biology and current status of translational research. Curr. Mol. Med. **9:**152–173.
29. **Tan, B. H., J. Fu, R. J. Sugrue, E. H. Yap, Y. C. Chan, and Y. H. Tan.** 1996. Recombinant dengue type 1 virus NS5 protein expressed in Escherichia coli exhibits RNA-dependent RNA polymerase activity. Virology **216:**317–325.
30. **Villordo, S. M., and A. V. Gamarnik.** 2009. Genome cyclization as strategy for flavivirus RNA replication. Virus Res. **139:**230–239.
31. **Yap, T. L., T. Xu, Y. L. Chen, H. Malet, M. P. Egloff, B. Canard, S. G. Vasudevan, and J. Lescar.** 2007. Crystal structure of the dengue virus RNA-dependent RNA polymerase catalytic domain at 1.85-angstrom resolution. J. Virol. **81:**4753–4765.
32. **Yoo, J. S., C. M. Kim, J. H. Kim, J. Y. Kim, and J. W. Oh.** 2009. Inhibition of Japanese encephalitis virus replication by peptide nucleic acids targeting cis-acting elements on the plus- and minus-strands of viral RNA. Antiviral Res. **82:**122–133.
33. **You, S., B. Falgout, L. Markoff, and R. Padmanabhan.** 2001. In vitro RNA synthesis from exogenous dengue viral RNA templates requires long range interactions between 5′- and 3′-terminal regions that influence RNA structure. J. Biol. Chem. **276:**15581–15591.
34. **You, S., and R. Padmanabhan.** 1999. A novel in vitro replication system for Dengue virus: initiation of RNA synthesis at the 3′-end of exogenous viral RNA templates requires 5′- and 3′-terminal complementary sequence motifs of the viral RNA. J. Biol. Chem. **274:**33714–33722.
35. **Yu, L., M. Nomaguchi, R. Padmanabhan, and L. Markoff.** 2008. Specific requirements for elements of the 5′ and 3′ terminal regions in flavivirus RNA synthesis and viral replication. Virology **374:**170–185.
36. **Zhang, B., H. Dong, D. A. Stein, P. L. Iversen, and P. Y. Shi.** 2008. West Nile virus genome cyclization and RNA replication require two pairs of long-distance RNA interactions. Virology **373:**1–13.
37. **Zhang, G., J. Zhang, A. T. George, T. Baumstark, and A. E. Simon.** 2006. Conformational changes involved in initiation of minus-strand synthesis of a virus-associated RNA. RNA **12:**147–162.
38. **Zhang, G., J. Zhang, and A. E. Simon.** 2004. Repression and derepression of minus-strand synthesis in a plus-strand RNA virus replicon. J. Virol. **78:**7619–7633.